Visible Light Response of Unintentionally Doped ZnO Nanowire Field Effect Transistors

ARTICLE *in* THE JOURNAL OF PHYSICAL CHEMISTRY C · SEPTEMBER 2009

Impact Factor: 4.77 · DOI: 10.1021/jp9046038

Visible Light Response of Unintentionally Doped ZnO Nanowire Field Effect Transistors

Yang Liu,[†] Zhiyong Zhang,[†] Huilong Xu,[†] Lihuan Zhang,[†] Zhenxing Wang,[†] Wenliang Li,[†] Li Ding,[†] Youfan Hu,[†] Min Gao,[†] Quan Li,[‡] and Lian-Mao Peng*,[†]

Key Laboratory for the Physics and Chemistry of Nanodevices and Department of Electronics, Peking University, Beijing 100871, China, Department of Physics, The Chinese University of Hong Kong, Shatin, New Territory, Hong Kong, China

Received: May 17, 2009; Revised Manuscript Received: July 20, 2009

A significant visible light response of unintentionally doped ZnO nanowire (NW) field effect transistors (FETs) has been observed in a reversible manner (for illumination source on and off). In particular, under white light illumination (wavelength longer than 400 nm), the threshold voltage (V_T) of the ZnO NW FET shifts greatly to the negative direction, suggesting a remarkable increase in carrier concentration. A photon-assisted oxygen molecule desorption mechanism is proposed to explain the observed sub-bandgap photoresponse on the basis of the behavior of the experimental devices in different gas atmospheres (air, vacuum, pure N_2, and pure O_2) and with/without nanowire surface modifications (coated with PMMA).

1. Introduction

ZnO is a direct wide band gap (~3.37 eV at room temperature) semiconductor with a large exciton binding energy (~60 meV).[1] ZnO nanostructures with diverse morphologies have been synthesized, including nanowires (NWs), nanobelts, nanotubes, nanosprings, nanocombs, and nanorings,[2] and their electrical and optical properties have been investigated.[2,3] Because of the excellent electrical and optical properties of ZnO NWs, these materials have been explored extensively for potential applications as field effect transistors (FETs),[4] piezoelectric devices,[5] light-emitting diodes,[6] ultraviolet (UV) detectors and lasers,[7−9] sensors,[2,10] and solar cells.[11] Because the band gap (E_g) of the ZnO NW is in the UV region, extensive investigations have been carried out on the UV response of the electrical characteristics of the ZnO NW. The large UV response is attributed to generations of electron−hole pairs across the band gap and efficient separation of electrons and holes due to band bending toward the surface of the ZnO NW.[7,8] Sub-bandgap response has also been observed in doped (by Al and Cu)[12,13] and unintentionally doped ZnO NWs[14−17] and attributed to generations of electron−hole pairs across the defect states and conduction/valence band. In this paper, we report the observation of significant visible light ($\lambda > 400$ nm) response on unintentionally doped ZnO NW-based FETs. We show, by carrying out a series measurements on the response of the ZnO NW FETs to white light irradiation under different environments, e.g., in air, vacuum, pure N_2, and pure O_2 gases, that our experimental results cannot be explained by the photon generation of the electron−hole pairs mechanism. Instead, we attribute the large visible light response to the photon-induced oxygen desorption from the surface of the ZnO NWs. With the oxygen ions being desorbed, the surface band bending is reduced and the depletion layer is narrowed, allowing a larger conduction channel for electrons to move from the source to the drain in the ZnO NW FET.

* To whom correspondence should be addressed. E-mail: lmpeng@pku.edu.cn.
[†] Peking University.
[‡] The Chinese University of Hong Kong.

2. Experimental Section

The ZnO NWs used in this study were synthesized by thermal evaporation of pure ZnO powder (99.99%) at 1200 °C. Microstructure and composition characterization were carried out using a FEI XL30 field emission gun scanning electron microscope (SEM) and a Tecnai 20 ST transmission electron microscope (TEM). Microphotoluminescence (PL) measurements were conducted using the 325 nm line of a He−Cd laser at room temperature. The as-grown ZnO NWs are typically n-type and have diameters ranging from 60 to 100 nm. To fabricate FETs, we dispersed ZnO NWs in ethanol and dropped them on degenerated Si substrate (used as a back gate electrode) covered with 200 nm thick thermally grown SiO_2 (used as an insulating gate oxide layer). Source and drain electrodes (50 nm Sc under 20 nm Pd) were fabricated via electron beam lithography and evaporation, followed by a standard lift-off process. Electrical measurements were carried out using a Keithley 4200 instrument and Janis cold stage at room temperature.

3. Results and Discussion

Figure 1a shows a high-resolution transmission electron microscopy (TEM) image of a typical ZnO NW, revealing an almost perfect crystal structure with little defects of line or plane type in the lattice. A typical microphotoluminescence (PL) spectrum measured from a single ZnO NW is shown in Figure 1b, in which a strong near-band edge (NBE) emission peaked at about 375 nm, and a very low green emission band (commonly accepted as originating from native point defects of ZnO) can be found. These results suggest that the ZnO NWs used in this work have high electronic structure quality. Figure 1c shows the scanning electron microscopy (SEM) image of a typical ZnO NW FET device. Two terminal electrical $I_{ds}-V_{ds}$ characteristics of the device are shown in Figure 1d with and without white light irradiation. The 18W commercial table lamp used in this study has a power spectrum (Figure 1e), and this spectrum shows four major emission peaks at 435, 485, 545. and 610 nm. All photoelectrical measurements were carried out by placing the lamp about 10 cm away from the device. The two curves in Figure 1d correspond to the $I-V$ characteristic of the device measured in air under white light irradiation (black

10.1021/jp9046038 CCC: $40.75
Published on Web 08/28/2009

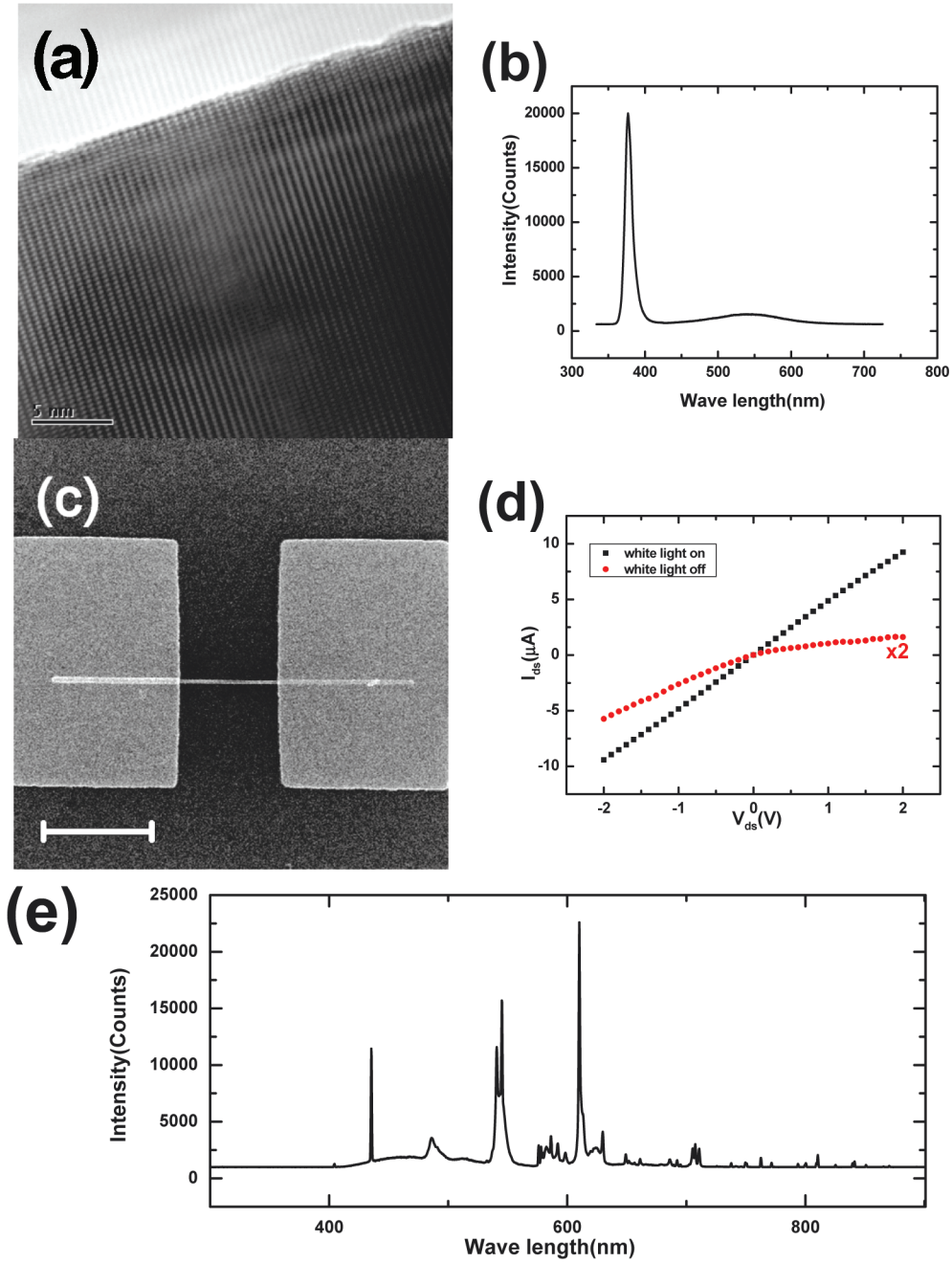

Figure 1. ZnO NWs and their optical and electrical characteristics. (a) High-resolution TEM image of the unintentionally doped ZnO NW, showing perfect lattice structure with little defects. Scale bar: 5 nm. (b) PL spectrum from a typical ZnO NW, showing a strong near-band edge emission. (c) SEM image of a typical ZnO NW-based FET device. The ZnO NW channel has a diameter of 80 nm and channel length of 1.9 μm. Scale bar: 2 μm. (d) Current−voltage ($I_{ds}-V_{ds}$) curves under white light illumination and 6 min after the lamp switched off. (e) Power spectrum of the white light lamp used in this work.

curve) and 6 min after the lamp was switched off (red curve), respectively. The almost linear $I-V$ curve (under white light irradiation) shows that the metal Sc electrode made good contact with the ZnO NW. After the light was switched off, the current dropped significantly. In particular, the current was suppressed for positive drain bias, and this effect may be attributed to the pinch-off effect, which restricts the device current.[10,15]

Figure 2a shows the field transfer characteristics of the back-gated ZnO NW FET (Figure 1c). The measurements were carried out for $V_{ds} = 1$ V and in air. The five curves in Figure 2a (and all similar characteristics) were all measured via varying the gate voltage V_{gs} from negative to positive and correspond to the conditions of light on and light off for 30 s; 3 min 20 s; 8 min 5 s; and 13 min 45 s, respectively, from left to right. Figure 2a clearly shows that under white light irradiation the ZnO NW FET is basically in its on state even for a very large negative $V_{gs} = -25$ V, and the FET starts to show n-type field characteristics when the white light is switched off. The threshold voltage V_T of the FET shifted from −19.7 to 4.3 V with time, i.e., the device was changed from depletion mode with $V_T < 0$ (shortly after the light was switched off) to enhancement mode with $V_T > 0$ (after the light was switched off for a long time). When the light was switched on again, the FET moved reversibly back into depletion mode (not shown). Similar threshold voltage shift behavior was also observed by Kim et al. under UV illumination.[18] Figure 2b shows the output characteristics of the device measured in the dark, and the different curves correspond to different gate voltages between

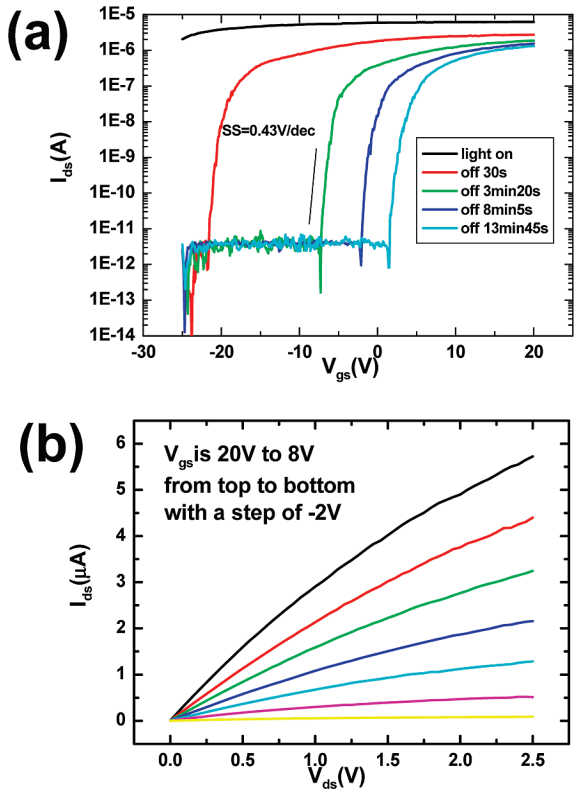

Figure 2. Electrical characteristics of a ZnO NW-based back-gated FET. (a) Field transfer characteristics of the ZnO NW FET (channel length $L = 1.9$ μm and NW diameter $d = 80$ nm) for $V_{ds} = 1$ V. Measurements were carried out in air and at different times after the white light lamp was switched on and off. (b) Output $I-V$ characteristics of the device in the dark, in which the gate voltage is varied from 20 to 8 V with a step of -2 V.

20 and 8 V with a step of -2 V, respectively. Relevant field transfer characteristics (similar to that shown in Figure 2a) show that the on/off current ratio is more than 10^6 at $V_{ds} = 1$ V (which is among the largest for back-gated ZnO NW FETs),[4] and the subthreshold swing, $SS = (dV_{gs})/[d(\log I_{ds})]$, is about 430 mV/decade (which is among the smallest for back-gated and uncoated ZnO NW FETs in air).[19,20] The gate capacitance of the ZnO NW FET can be estimated to be about 1.66×10^{-16} F using a cylinder on plate model $C = (2\pi\varepsilon_0\varepsilon_r L_{NW})/\{\ln[2(h + r_{NW})/r_{NW}]\}$, where $\varepsilon_r = 3.9$ is the relative dielectric constant, $h = 200$ nm is the thickness of the SiO_2 dielectric layer, and r_{NW} is the radius of the ZnO NW. The transconductance, $g_m = (dI_{ds})/(dV_{gs})$, is estimated to be about 98 nS at $V_{ds} = 1$ V. In addition, electron mobility and electron concentration can be obtained via equations $\mu = (g_m L^2)/(CV_{ds})$ and $n = 1/(e\rho\mu)$, yielding $\mu = 21 \text{cm}^2/\text{V s}$ and $n = 6 \times 10^{17} \text{cm}^{-3}$ for the device after the white light was switched off for 6 min.

The as-grown ZnO NW is normally a n-type semiconductor. Because the NW has a large surface/bulk ratio and a depletion length that is comparable to its diameter, its conductivity depends sensitively on the charged molecules absorbed onto its surface.[21] This is because the negatively charged surface molecules will cause a surface band bend upward, resulting in a depletion layer at the surface of a n-type semiconductor, and this in turn will lead to a conductance decrease of the device. However, desorption of the negatively charged surface molecules will release the band bending and increase the conductance of the ZnO NW.[21] We attribute the observed significant conductance change as well as the threshold voltage shift on white light irradiation to the photon-assisted desorption of the chemically adsorbed molecules and their readsorption in the dark. The negatively charged ions adsorbed on the surface of the ZnO NW will widen the depletion region and decrease the current, so a more positive gate voltage is needed to shift the conduction band down toward the Fermi level to turn the FETs on, resulting in a positive shift of the threshold voltage after the light was switched off (Figure 2a).

In order to find out what kind of molecules were adsorbed on the surface of the ZnO NW and contributed to the sub-bandgap photoresponse, we carried out electrical transport measurements on the ZnO NW FETs in different gas atmospheres. Figure 3a illustrates the time response of the current measured in air and in vacuum (10^{-2} Pa) with the white light alternately being switched on and off. We define the risetime T_r as the time needed for the current to rise from the dark current level to $(1 - e^{-1})$ its maximum level (I_{max}), and the decay time T_d as the time needed for the current to drop to $I_{max}e^{-1}$. In air and in vacuum, the current increased greatly (more than 10^3 times) when the light was switched on, and the risetime is estimated to be around 40 s in air and 42 s in vacuum. When the light was switched off, the current decreased immediately, and the decay characteristic time is about 84 s in air and 400 s in vacuum. Figure 3a shows clearly that the current drops faster and to smaller values in air than in vacuum after the light was switched off. In addition, the current failed to return to its initial value in vacuum after the light was switched off for hundreds of seconds. This is because while molecules can be desorbed quickly from the surface of the ZnO NW on the irradiation of energetic photons in air and in vacuum alike, readsorption of these molecules back onto the surface of the ZnO NW depends very sensitively on the availability of the molecules in the atmosphere. As a result, recovering in air is much easier than in vacuum, leading to a longer T_d in vacuum than in air. It should be noted that molecule desorption and adsorption occur simultaneously on the surface of the ZnO NW, and a stable current will be observed only when an equilibrium is reached between the two events, i.e., when the rate of desorption equals that of adsorption. Because the number of molecules in vacuum is much less than that in air, the maximum current under white light irradiation in vacuum is larger than that in air, and the off state current cannot recover to its initial value. Because after each cycle there exists fewer molecules on the surface of the ZnO NW, the maximum current became larger after each cycle of switching the light on and off and before equilibrium was reached. Figure 3b shows the field transfer characteristics of the same device as that shown in Figure 2a in vacuum for $V_{ds} = 1$ V. It is clearly shown that the transport characteristic recovering is much slower in vacuum than in air after the light was switched off, and again, this is due to the rather limited number of molecules that were available around the ZnO NW for readsorption in vacuum.

Because air is mainly composed of nitrogen (78%) and oxygen (21%), we further investigated the response of the ZnO NW FETs to nitrogen and oxygen. As shown in Figure 3c, the current did not show obvious change when nitrogen of high purity was introduced into the vacuum chamber at $t = 300$ s. Nevertheless, it increased rapidly when the white light was switched on and dropped again when the light was switched off. The risetime $T_r \sim 62$ s and decay time $T_d > 400$ s were observed, and these characteristic times are similar to that found in vacuum as shown in Figure 3a, indicating that nitrogen was not the molecule that caused a major influence on the conductivity of the ZnO NWs. However, the current dropped immediately when high-purity oxygen was introduced, and the light

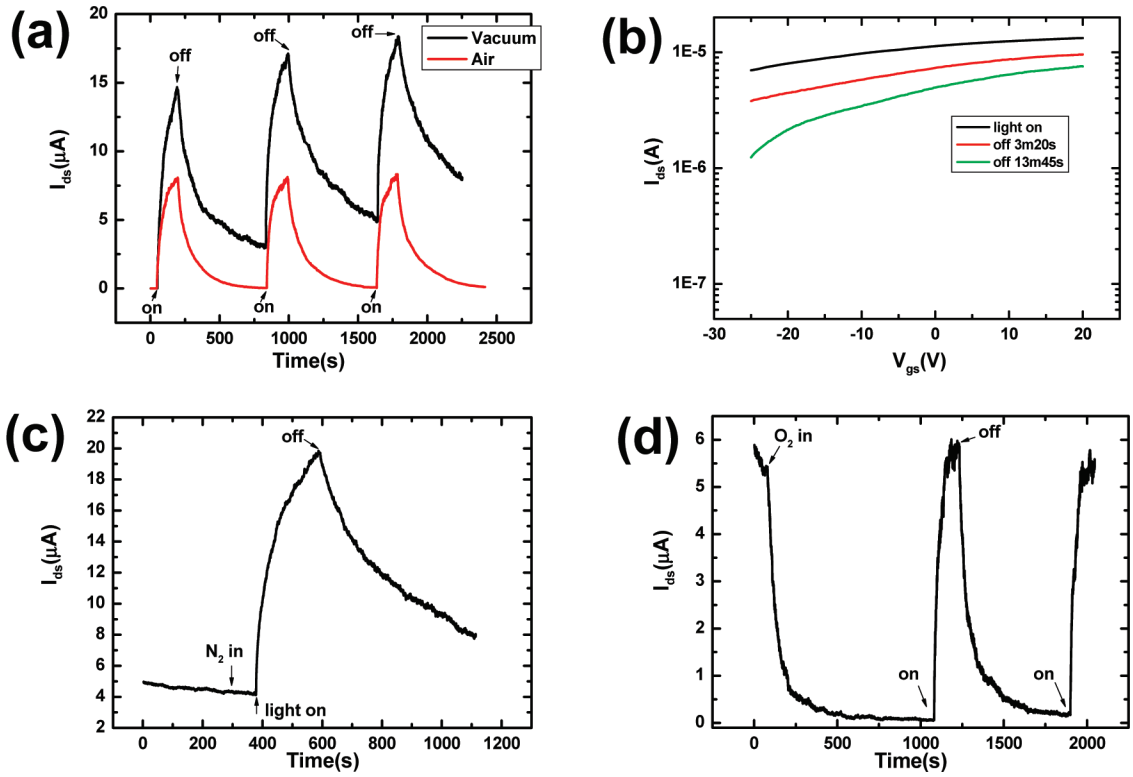

Figure 3. Device current variation with environment. (a) Time response of the current measured in air and in vacuum (10^{-2} Pa) with the white light being alternately switched on and off for $V_{ds} = 2$ V. (b) $I_{ds}-V_{gs}$ curves of the back-gated ZnO NW FET measured in vacuum at different times after the lamp was switched off for $V_{ds} = 1$ V. (c) Time response of the current measured in vacuum chamber but with N_2 being introduced and white light being switched on and off for $V_{ds} = 2$ V. N_2 was introduced in vacuum at about 300 s. (d) Similar time response of the device as panel c but with O_2 being introduced into the chamber at about 100 s.

response of the device was quite similar to that in air (Figure 3d), with $T_r \sim 27$ s and $T_d \sim 52$ s, both smaller than that in air. This shorter response time is due to the higher oxygen concentration than that in air. The $I_{ds}-V_{gs}$ curve measured in oxygen at the light off condition showed that the ZnO NW device exhibited gate modulation (Figure S1 of the Supporting Materials) similar to that measured in air. Because the polymethyl methacrylate (PMMA) layer does not allow water molecules to permeate through it,[22,23] we also examined the PMMA-coated ZnO NW FETs. Significant sub-bandgap response is also observed on these PMMA-coated ZnO NW FETs (Figure S2 of the Supporting Materials), confirming that water molecules are not responsible for this effect. We thus conclude that it is the oxygen molecules whose adsorption and desorption caused significant change in the conductance and threshold voltage shift of the ZnO NW FET. When the oxygen molecule is adsorbed onto the ZnO surface, an electron is transferred from the NW to the oxygen molecule to form chemisorbed O_2^-, resulting in a surface depletion layer that decreases the NW conductance. When the chemisorbed negatively charged ions are desorbed from the surface, the depletion layer becomes conductive again and conductance increases.[10,21]

A similar sub-bandgap light response on unintentionally doped ZnO was indeed observed and reported earlier.[14−17] The ZnO NWs or epilayers examined in refs 14−16 had a strong green band emission, indicating that the ZnO samples had a high defect density making them unlikely to exhibit a strong field effect and therefore suitable for FET applications. However, the ZnO NWs examined in this work have a very weak green band emission (Figure 1b), suggesting a much lower defect density associated with the green emission.[17] Earlier studies showed that chemical adsorption occurs much easier at oxygen vacancies, which are the dominant defects on the ZnO surface.[24] The actual coverage of chemisorbed O_2^- on the surface is typically less than 2.5×10^{-4} monolayer, but it was shown that even such a small coverage of O_2^- is sufficient to change the conductivity of undoped ZnO.[24] While our ZnO NWs have relatively low defect densities, the oxygen ions chemically adsorbed onto the surface of the ZnO NW have a sufficient effect on the conductance of the ZnO NW, yielding a low green band emission (Figure 1b), strong field effect, and sub-bandgap photoresponse at the same time (Figure 2a). Because the depletion length (typically tens of nanometers) is comparable with the NW diameter, the ZnO NW is fully depleted by the surface oxygen chemisorption, pushing the FET to its off state at zero gate bias. A positive gate voltage is then needed to shift the conduction band down toward the Fermi level to open the conduction channel, leading to a positive threshold voltage (Figure 2a).

To summarize the photon response of ZnO NW, we depict in Figure 4 three distinct mechanisms. Typically the as-grown ZnO NWs are n-type, having certain O_2^- ions being adsorbed onto their surface. These chemically adsorbed ions bend the band structure of the ZnO NW near its surface, creating a depletion shell around the ZnO NW as shown in Figure 4a. Under the irradiation of photons of sufficient energy ($E_p > E_g$), electron−hole pairs are generated over the band gap of the ZnO NW. While holes migrate toward the surface via the electrostatic field resulting from surface band bending, electrons in the inner core of the ZnO NW contribute directly to photocurrent, and this explains the well-established UV photoconductivity of the ZnO NWs.[7,8] For an intentionally doped NW, if the associated energy levels E_d are situated in the band gap below the conduction band such that $E_c - E_d \gg k_B T_{RT}$,[12,13] with k_B being

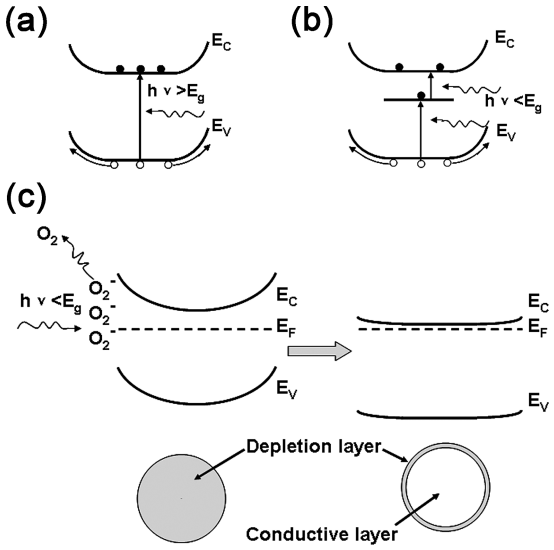

Figure 4. Schematic diagrams showing the band structure and UV and sub-bandgap photoresponse mechanisms of ZnO NWs. (a) UV photoresponse with photon energy larger than the band gap. Sub-bandgap photoresponse with photon energy less than the band gap for (b) intentionally doped ZnO and (c) unintentionally doped ZnO. The surface adsorbed oxygen molecules caused band bending and full depletion of the ZnO NW. This depletion is reduced to partial depletion when some oxygen ions are being desorbed from the surface via the assistance of the incident photons with energy larger than the surface oxygen binding energy ~1.1 eV.

the Boltzmann constant and T_{RT} the room temperature, electron−hole pairs can be generated by sub-bandgap excitation (Figure 4b), contributing to the sub-bandgap response of the ZnO NWs. However, for the unintentionally doped ZnO NWs, $E_c - E_d \sim k_B T_{RT}$, the electron−hole pair mechanism for the sub-bandgap response does not work. This is because at room temperature almost all relevant donor levels are thermally excited and additional excitation with photons of sub-bandgap energy does not contribute significantly to the conductance of the ZnO NW. Here, in Figure 4c, we depict a new mechanism for explaining the sub-bandgap photon response of unintentionally doped ZnO NWs.

For unintentionally doped ZnO NWs such as the ones used in this work, because there exist little defects in the NWs associated with green emission, photons with energy less than the band gap cannot generate a large quantity of electron−hole pairs. However, it is a well-established fact that the activation energy (E_a) for oxygen desorption from the ZnO surface is about 1.0−1.1 eV.[25] Figure 4c shows a photon-assisted molecule desorption (PAMD) mechanism for sub-bandgap photon response. While photons with energy larger than the surface oxygen binding energy but smaller than the band gap of the ZnO NW cannot generate a large quantity of electron−hole pairs, they can release the chemisorbed oxygen ions on the surface of the ZnO NW. On releasing the negatively charged oxygen ions, the surface depletion shell is narrowed and the inner conduction channel is opened, resulting in increased conductivity of the ZnO NW device.

To further verify our PAMD mechanism, we chose monochromatic light (633 nm He−Ne laser, power density ~10^3W/cm^2) with low photon energy to repeat the sub-bandgap response experiment. Figure 5a shows the field transfer characteristics of another typical back-gated ZnO NW FET for $V_{ds} = 1$ V and in air. The four curves in Figure 5a were all measured via varying the gate voltage V_{gs} from negative to positive and correspond to the conditions of laser on and laser off for 30 s;

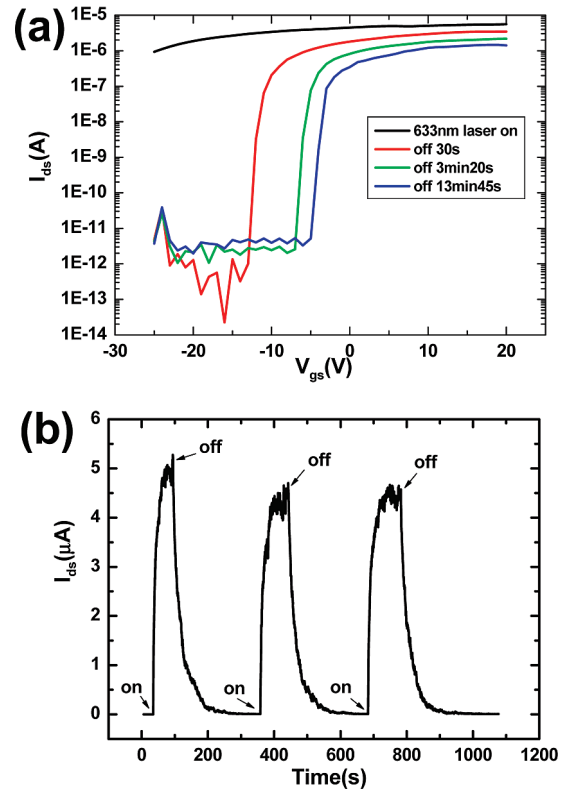

Figure 5. Electrical characteristics of another typical ZnO NW-based back-gated FET. (a) Field transfer characteristics of the ZnO NW FET for $V_{ds} = 1$ V. Measurements were carried out in air and at different times after the 633 nm He−Ne laser (power density ~10^3W/cm^2) was switched on and off. (b) Time response of the current measured in air with the 633 nm He−Ne laser being alternately switched on and off for $V_{ds} = 2$ V.

3 min 20 s; and 13 min 45 s, respectively, from left to right. Similar to Figure 2a, the ZnO NW FET under 633 nm laser irradiation is basically in its on state even at the largest negative gate voltage ($V_{gs} = -25$ V). When the laser is switched off, the FET starts to show n-type semiconductor behavior, and the threshold voltage is shifted from the negative side to the positive side. Figure 5b shows the time-dependent current response to the laser beam irradiation in air at $V_{ds} = 2$ V. The on/off current ratio is more than 10^3, and the risetime T_r and decay time T_d are estimated to be about 10 s and 22 s, respectively. This time-dependent current response is similar to that shown in Figure 3 but with different characteristic times, T_r and T_d, which can be attributed to the difference in the two ZnO NW FETs (such as different surface conditions and threshold voltages[18]). The photons from the 633 nm laser have energy of 1.96 eV, which is larger than the binding energy of chemisorbed oxygen but smaller than the band gap of ZnO and that associated with all main emission peaks of the white light source used earlier (Figure 1e). As a result, the photons have enough energy to assist desorption of the chemisorbed oxygen ions from the surface but not enough to excite a significant amount of electron−hole pairs. Figure 5 shows a significant photoresponse, suggesting that the sub-bandgap response results from oxygen desorption and absorption.

4. Conclusions

A significant visible light response of unintentionally doped ZnO NW-based FETs has been observed, and the threshold voltage is found to shift greatly from 4.3 V (enhancement mode) to less than

−25 V (depletion mode) under white light illumination. The device photoresponse in different gas atmospheres (ambient air, vacuum, pure N_2, and pure O_2) suggests that adsorption and desorption of oxygen molecules on the nanowire surface greatly changes the conductance as well as the V_T of NW FETs. A photon-assisted molecule desorption mechanism is proposed to explain this sub-bandgap photoresponse.

Acknowledgment. This work was supported by the Ministry of Science and Technology (Grant 2006CB932401) and National Science Foundation of China (Grant 90606026). Q.L. acknowledges the GRFs grant from RGC of HKSAR (Project 402007 and 414908) and the CUHK Focused Investments Scheme C.

Supporting Information Available: Field transfer characteristics of the back-gated ZnO NW FET in O_2 and PMMA coating effects of the electrical characteristics of the ZnO NW-based FET. This material is available free of charge via the Internet at http://pubs.acs.org.

References and Notes

(1) Özgür, Ü.; Alivov, Y. I.; Liu, C.; Teke, A.; Reshchikov, M. A.; Doğan, S.; Avrutin, V.; Cho, S.-J.; Morkoç, H. *J. Appl. Phys.* **2005**, *98*, 041301.
(2) Wang, Z. L. *J. Phys.: Condens. Matter* **2004**, *16*, R829.
(3) Djurisic, A. B.; Leung, Y. H. *Small* **2006**, *2*, 944.
(4) Chang, P.-C.; Lu, J. G. *IEEE Trans. Electron Devices* **2008**, *55*, 2977.
(5) Wang, Z. L.; Song, J. *Science* **2006**, *312*, 242.
(6) Bao, J.; Zimmler, M. A.; Capasso, F.; Wang, X.; Ren, Z. F. *Nano Lett.* **2006**, *6*, 1719.
(7) Kind, H.; Yan, H.; Messer, B.; Law, M.; Yang, P. *Adv. Mater.* **2002**, *14*, 158.
(8) Soci, C.; Zhang, A.; Xiang, B.; Dayeh, S. A.; Aplin, D. P. R.; Park, J.; Bao, X. Y.; Lo, Y. H.; Wang, D. *Nano Lett.* **2007**, *7*, 1003.
(9) Huang, M. H.; Mao, S.; Feick, H.; Yan, H.; Wu, Y.; Kind, H.; Weber, E.; Russo, R.; Yang, P. *Science* **2001**, *292*, 1897.
(10) Fan, Z.; Wang, D.; Chang, P.-C.; Tseng, W.-Y.; Lu, J. G. *Appl. Phys. Lett.* **2004**, *85*, 5923.
(11) Leschkies, K. S.; Divakar, R.; Basu, J.; Enache-Pommer, E.; Boercker, J. E.; Carter, C. B.; Kortshagen, U. R.; Norris, D. J.; Aydil, E. S. *Nano Lett.* **2007**, *7*, 1793.
(12) Lin, D.; Wu, H.; Pan, W. *Adv. Mater.* **2007**, *19*, 3968.
(13) Kouklin, N. *Adv. Mater.* **2008**, *20*, 2190.
(14) Keem, K.; Kim, H.; Kim, G.-T.; Lee, J. S.; Min, B.; Cho, K.; Sung, M.-Y.; Kim, S. *Appl. Phys. Lett.* **2004**, *84*, 4376.
(15) Fan, Z.; Chang, P.-C.; Lu, J. G.; Walter, E. C.; Penner, R. M.; Lin, C.-H.; Lee, H. P. *Appl. Phys. Lett.* **2004**, *85*, 6128.
(16) Moazzami, K.; Murphy, T. E.; Phillips, J. D.; Cheung, M. C.-K.; Cartwright, A. N. *Semicond. Sci. Technol.* **2006**, *21*, 717.
(17) Li, Q. H.; Gao, T.; Wang, Y. G.; Wang, T. H. *Appl. Phys. Lett.* **2005**, *86*, 123117.
(18) Kim, W.; Chu, K. S. *Phys. Status Solidi A* **2009**, *206*, 179.
(19) Chang, P.-C.; Fan, Z.; Chien, C.-J.; Stichtenoth, D.; Ronning, C.; Lu, J. G. *Appl. Phys. Lett.* **2006**, *89*, 133113.
(20) Song, S.; Hong, W.-K.; Kwon, S.-S.; Lee, T. *Appl. Phys. Lett.* **2008**, *92*, 263109.
(21) Hu, Y. F.; Liu, Y. ; Li, W. L.; Gao, M.; Liang, X. L. ; Li, Q.; Peng, L.-M. *Adv. Func. Mater.* **2009**, in press.
(22) Kim, W.; Javey, A.; Vermesh, O.; Wang, Q.; Li, Y.; Dai, H. *Nano Lett.* **2003**, *3*, 193.
(23) Javey, A.; Wang, Q.; Kim, W.; Dai, H. *Tech. Dig. IEEE Int. Electron Devices Meet.* **2003**, 741.
(24) Henrich, V. E.; Cox, P. A. *The Surface Science of Metal Oxides*; Cambridge University Press: New York, 1994, pp 148, 298.
(25) Watanabe, H.; Wada, M.; Takahashi, T. *Jpn. J. Appl. Phys.* **1965**, *4*, 945.

JP9046038